A MULTI-VIEW STEREO SYSTEM FOR ARTICULATED MOTION ANALYSIS

Francesco Setti, Mariolino De Cecco
Department of Structural and Mechanical Engineering, University of Trento, via Mesiano 77, Trento, Italy

Alessio Del Bue [*]
Istituto Italiano di Tecnologia, Via Morego 30, 16163 Genova, Italy

Keywords: Human motion analysis, Multi-view stereo, 3D reconstruction, Motion segmentation.

Abstract: In this paper we present a system for the motion segmentation of a human arm and the determination of its internal joint characteristics (position and degrees of freedom). In particular, we are interested in the segmentation of a set of 3D points lying over a pair of non-rigid bodies (arm and forearm) connected through a rotational joint (elbow). The complexity of the problem resides in the non-rigidity of the motion given by the human articulations and the soft tissues of the body (e.g. skin and muscles). In this work we address the aspects of 3D reconstruction by multi-stereo vision, frame-by-frame matching of the feature points, motion segmentation and the joint characteristics determination.

1 INTRODUCTION

The interest on 3D reconstruction and motion analysis devices is growing due to the wide application of these systems in different industrial and scientific fields. The recent advancements in Computer Vision have impacted highly in the movie and advertisement industries (Boujou, 2009), in the medical analysis area, in video-surveillance applications (Ioannidis et al., 2007) and in biomechanics studies of the human body (Corazza et al., 2007; Fayad et al., 2009). However, the strongest limitation for several systems is their restriction to deal with rigid bodies only. A shape which is deforming introduces new challenges, the object can vary arbitrary and the observed shape may have different articulations not known a priori.

The vision system here developed is tuned to tackle such problems. It consists of a set of twelve cameras in a stereo pair setup (see Figure 1) and a special pattern with distinctive markers to overlay over the subject. Our application is driven towards the analysis of human motion but it is general in his concept and applicable to different shapes. Given the pattern and multiple views the proposed vision system is able to:

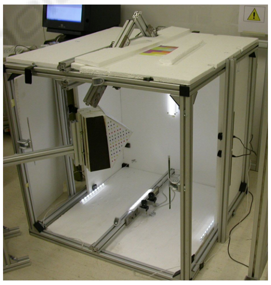

Figure 1: The image acquisition system used in our experiments.

- For each frame obtain a 3D reconstruction given the markers position;
- Match 3D points at each pair of frames given the repetitive structure of the marker pattern;
- Segment articulated body parts if such motion exists;
- Compute the joint position of the two bodies.

The final aim of our system is to describe the full articulated body in 3D and to infer its motion properties automatically from a set of images given a known pattern. Our application domain is the analysis of the manipulation skill of humans where accurate measurements of the articulation are fundamental.

[*]This work was partially supported by Delta R&S, Fundação para a Ciência e a Tecnologia (ISR/IST pluri-annual funding) through the POS_Conhecimento Program (include FEDER funds) and grant MODI-PTDC/EEA-ACR/72201/2006. A special thanks to João Fayad for helpful suggestions.

Setti F., De Cecco M. and Del Bue A. (2010).
A MULTI-VIEW STEREO SYSTEM FOR ARTICULATED MOTION ANALYSIS.
In *Proceedings of the International Conference on Computer Vision Theory and Applications*, pages 367-372
DOI: 10.5220/0002847303670372

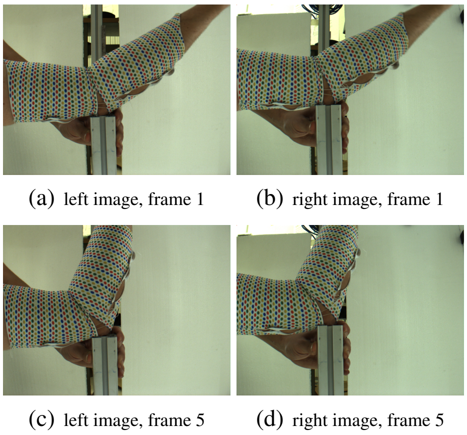
(a) left image, frame 1 (b) right image, frame 1

(c) left image, frame 5 (d) right image, frame 5

Figure 2: An example of a set of images acquired from the stereo-pairs.

This paper first describes the image acquisition system and the 3D reconstruction process in Section 2. The next Section 3 shows how the pairwise 3D matching is done exploiting the particular structure of the pattern. Section 4 presents the segmentation algorithm based on the motion of the object shape. Section 5 describes the articulated joint position computation and finally Section 6 presents some real experimental results with a bending arm. Section 7 finally proposes a discussion of the system.

2 IMAGE ACQUISITION AND 3D RECONSTRUCTION

The image acquisition system is able to reconstruct the position of a set of points belonging to a generic surface located in a given working space. The related software manages 12 cameras, connected in a configuration of 6 stereo-pairs. The camera model parameters are estimated through camera calibration and an accurate description of this stage can be found in (De Cecco et al., 2009).

Figure 2 shows the 3D reconstruction for the first and last frame acquired from the system for an eight frame long sequence. The reconstruction procedure is based on the acquisition of color markers superimposed on the shape by means of a wearable cloth. Marker matching between cameras is performed using both epipolar geometry and pattern geometry to minimize outliers. In particular the pattern is a sequence of alternate stripes of color markers of four different colors (red, green, yellow and blue).

We employ a cloth on which a pattern of markers is painted. There are other systems that make use of artificial markers on cloths. (Scholz and Magnor, 2006) use a circular patterns of five different colors similar to the one used in our setup. (White et al., 2007) adopt a mesh of triangular geometric shapes with random colors. One of the main challenges is the correct matching of each marker. In our case we use a highly symmetric aligned pattern of circular markers as shown on the arm in figure 2. Correspondences are solved by first clustering the lines and than searching for the best matches between lines. Although more computation is needed we believe this method is more robust when dealing with high curvature objects and when the lighting conditions are not optimal (White et al., 2007).

Each stereo pair provides the depth evaluation of each point in the field of view; a compatibility analysis between points reconstructed from more than one stereo pair is performed by using Mahalanobis distance and the fusion of compatible points is performed employing a Bayesian approach (De Cecco et al., 2009). The output of the 3D reconstruction stage is a $n \times 5$ matrix M for each frame such that:

$$M = \begin{bmatrix} x_1 & y_1 & z_1 & col_1 & unc_1 \\ \vdots & \vdots & \vdots & \vdots & \vdots \\ x_n & y_n & z_n & col_n & unc_n \end{bmatrix}$$

where n is the number of reconstructed points. The first three columns of M are the 3D coordinates x, y and z of the point. The fourth column is a scalar that indicate the color of the marker while the last one is a scalar that gives the uncertainty of the reconstructed point. Figure 3 shows an example of the 3D reconstruction for an eight frames image sequence where the captured non-rigid motion is an arm bending as presented in Figure 3 using a single stereo pair view.

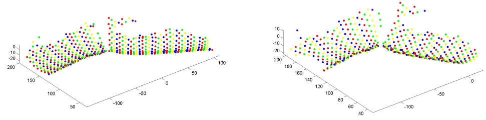

Figure 3: The left and right image shows the first and last frame respectively of the eight frame sequence used for the 3D reconstruction of the human arm.

3 TRAJECTORY MATRIX

The previous reconstruction stage provides a set of unordered 3D coordinates at each image frame. The next task is to match each 3D point in a given frame the corresponding 3D point in the following frame. This is a fundamental step in order to infer the global properties of the non-rigid image shape (i.e. its motion). This 3D matching stage aims to form a complete measurement matrix W in which each column of the matrix represents the 3D trajectory of a point. As an example, consider the first two frames of a sequence. After $3D$ reconstruction we have two matrices M_1 and M_2 with n and m points where in general $n \neq m$. The output of the frame-by-frame points matching algorithm is a vector

$$P^2 = \begin{bmatrix} P_1^2 \\ \vdots \\ P_n^2 \end{bmatrix}$$

with the same number of rows of the matrix M_1, each row contains the index of the point in the second frame matched with the one in the first frame. If a point of the first frame has no given assignment in the second frame, the value in P^2 will be NaN.

3.1 Matching using Nearest Neighbor

Our main contribution is to propose a set of matching algorithms robust to non-rigid deformations using the properties of the given pattern. One of the simplest algorithm we can use is a revisited version of the classical Nearest Neighbor (NN) approach to account for the different color assigned to each 3D point in both frames. The algorithm is composed by the steps below:

1. Compute the metric distance matrix between each pair of points of the same color in the two frames; the pairs of points of different colors the correspondent value is NaN.
2. Compute the minimum distance for each point of $frame_1$ where NaN values are ignored. We obtain a $n \times 2$ matrix D_{min} where the columns represent the minimum distance and the index of the nearest point.
3. If the minimum distance between two points is lower than a threshold and the association is unique, the association is considered valid, otherwise it will be deleted.

The threshold is automatically computed from the mean distance, the mean of the first column of the matrix D_{min}, multiplied by a coefficient. This algorithm gives reasonable results under the hypothesis that the movement of the feature between two successive frames is small with respect to the distance between the features in a single frame. This means that the motion of the bodies is tiny with respect to the frame rate and the features spatial density.

3.2 Matching using NN and Procrustes Analysis

We also propose to combine NN and Procrustes Analysis (PA) theory. The algorithm is composed by the three distinctive stages.

1. Stripe Sorting. Given the pattern repetitive structure, it is possible to associate points with the same color to a set of stripes. Each stripe is sorted along the principal directions of the 3D shape at the given frame.

2. Stripe Matching. In this stage we match each stripe in the first frame to a stripe in the second frame. This association is made using a NN approach on the centroid of each stripe using again the color as a discriminative feature.

3. Match 3D Points in Each Stripe. For two matched stripes, we select first the stripe containing less 3D points. Then we sequentially assign these points to the 3D points of the other stripe and we register the two sets using PA (Kanatani, 1996) (Figure 4 shows a graphical explanation). We selected the assignment which results in the minimum 3D error after registration.

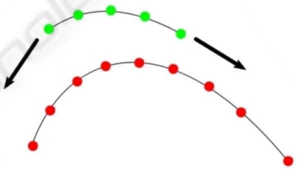

Figure 4: The points on the top line slide over the point of the bottom line. At each slide, registration with PA is made with the corresponding points. The 3D residual between the registered set of points is then used as the criteria for the best match.

Stage 1 and 2 are based on the observation that a NN over the centroid of the stripes is more robust to deformation and more computationally efficient than performing a NN on each 3D point. Especially for the second step, if the deforming body can be considered locally rigid on the stripe, the rigid registration by PA give low 3D residual if the matching is correct.

The proposed algorithm is very robust for short movements with respect to the stripe-by-stripe distance. If the displacement between the centroids of the same stripe in two following frames is comparable to the stripe-by-stripe distance, this method is no longer robust. In this case we can use a similar algorithm, *Local Procrustes Analysis* (LPA), in which we consider not only the associated stripe for the PA, but also the n-nearest. This method is more robust than the previous one in the case of large displacements. Unfortunately this modification introduces more sensibility to deformations.

Once we have a frame-by-frame matching array for each pair of successive frames, we can build a trajectory matrix W taking into account only the features tracked in all the frames. The trajectories of the full tracked points in the example case are shown in Figure 5. In this algorithm we consider only the points tracked in all the frames, the markers tracked only in a few frames could be considered with a dedicated missing data algorithm.

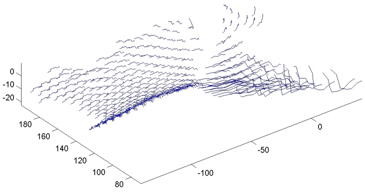

Figure 5: The 3D point matching between five successive frames.

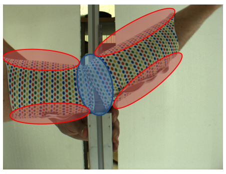

Figure 6: The expected critical zone in the segmentation stage: the border zone (blue) and the joint zone (red).

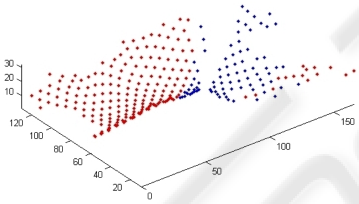

Figure 7: Human arm segmentation using the Generalized Principal Component Analysis (GPCA).

4 MOTION SEGMENTATION

Once the matching problem is solved, the matrix W stores the correct temporal information of the 3D trajectories of the non-rigid body. In order to compute the location of a joint, we need now to segment the full non-rigid 3D motion into a subset of relevant rigid motions. In the experimental case here presented this means to assign each 3D trajectory in W to two clusters of points lying on the forearm and on the arm. In the following section we evaluated the results obtained by a subset of these methods applied and modified for the 3D segmentation problem. In particular, we assess the performances of three algorithms: Generalized Principal Component Analysis (GPCA) (Vidal et al., 2005), Subspace RANSAC (Fischler and Bolles, 1987; Tron and Vidal, 2007) and Local Subspace Affinity (LSA) (Yan and Pollefeys, 2008).

These algorithms obtains reasonable results for 2D motion segmentation tasks with the LSA approach obtaining the best results (Tron and Vidal, 2007). In the following, we evaluate their quality with bodies that show a certain degree of non-rigidity and soft tissue artifacts. In general, we expect decreasing performance in two different regions:

border zone where the marker's movement could be affected by the muscle tension. Regions are marked with blue in Figure 6.

joint zone where the two bodies are not well separated because of the geometrical conformation of the natural joint (elbow). The region is marked with red in Figure 6.

4.1 GPCA Algorithm

The GPCA (Vidal et al., 2005) method was introduced with the purpose of segmenting data lying on multiple subspaces. This is also the case for 3D shapes moving and articulating since their trajectories lie on different subspaces. The method is algebraic and it first fits the union of the subspaces to a set of polynomials with a certain degree. Then subspaces are clustered using the derivative at a point which gives the normal to the subspace containing the point. Figure 7 shows the segmentation results using GPCA over the arm movement 3D data. The segmentation error is about 25% in this test showing several outliers far from the joint and thus from the expected regions. This unexpected result may be a consequence of the non-rigid motion of the body parts.

4.2 RANSAC Algorithm

The method is based on the selection of the best model which fit the inlier data. In order to estimate the putative models, candidates set of points are chosen randomly and then the residual given the fitted model is stored. After several random sampling, the model which fits best the inliers is chosen. For our case, this algorithm is the worst performing of the three obtaining a segmentation error of approximately 50% of the given points for this dataset. Figure 8 shows that most of the errors are located at the border zone, where we expect errors because the movement of the markers could be affected by the muscle tension. This method gives errors in both the expected regions, joint and border, but in general we have several errors also in similar critical region as for the GPCA algorithm.

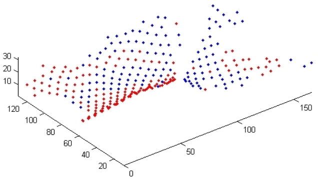

Figure 8: Human arm segmentation using the RANSAC.

4.3 LSA Algorithm

The LSA approach (Yan and Pollefeys, 2008) uses spectral analysis in order to define the data clusters which refer to different motion subspaces. It is based on local subspace fitting in the surrounding of each trajectory followed by spectral clustering. Figure 9 shows that the LSA algorithm is the best performing between the tested three with a total segmentation error of about 8%. The algorithm correctly estimate the points in the border zone, but we have few errors in the joint zone. Interestingly, the mistakes out of the critical expected regions are rather few. This is probably related to the fact that the LSA algorithm is more robust to the noise possibly introduced by soft-tissue artifacts than the other two considered approaches.

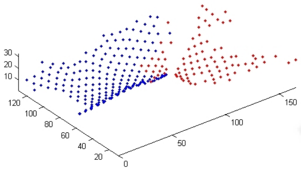

Figure 9: Human arm segmentation using the Local Subspace Affinity (LSA).

5 JOINT RECONSTRUCTION

The theoretical property used to perform the computation of the joint is that the subspaces computed from the trajectories of two body parts intersects. Such common intersection can be used to identify the joint position and properties as noticed by (Yan and Pollefeys, 2008; Tresadern and Reid, 2005) for image data and used by (Fayad and P. M. Q. Aguiar, 2009) for 3D data. We use the computational tool developed in the latter work to perform the estimation of the joint position.

In this stage we have two critical aspects. First, outliers after the segmentation stage may cause instability in the estimation of the joint. The second problem is the planarity of the reconstructed points; in this case the configuration would be degenerate thus introducing some instability in the computation of the joint position and sensibility to noise, and so the computation of some internal steps of the algorithm can be affected from matrix rank deficiency. One more critical point in this case is the co-planarity of the points and the motion.

6 EXPERIMENTAL RESULTS

For the evaluation of this framework we developed two experiments. In the first, we used two exactly rigid bodies (two boxes) linked by a mechanical joint. This setup has the aim to test the system performance when there are no soft tissue artifacts. In the second we tested our system using a real human arm.

Figure 10 resumes the results for the first test. The sequence is composed from 15 frames acquired from 2 stereo pairs; matching is performed by using the novel algorithm that combine NN and PA. The segmentation using LSA algorithm gives a segmentation error of only 1% given the ground truth showing the good performance of this method with rigid bodies.

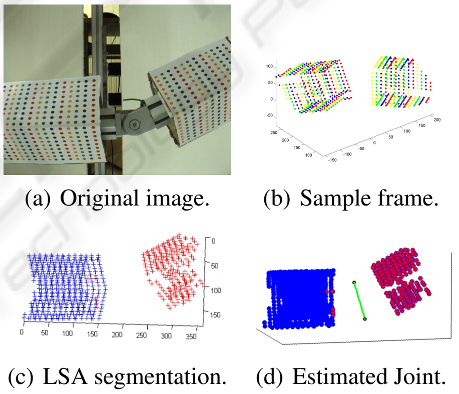
(a) Original image. (b) Sample frame.

(c) LSA segmentation. (d) Estimated Joint.

Figure 10: The first experiment setup. The images show: a) a sample frame, b) a reconstructed frames, c) the segmentation result using LSA and d) the estimated axial joint (red).

In the second experiment we have acquired a sequence of a human arm performing a bending movement and Figure 11 resumes the results. In this case we used a sequence of 8 frames acquired from a single stereo pair. The matching is performed again with the combined NN and PA. The total segmentation error using LSA algorithm is about 8%. Figure 11(d) shows the estimated rotational joint, the 3D position of the elbow. The first approximation of the human elbow is an axial joint, this is a good model when we consider a low number of feature points; in this case we have over 300 feature points near the elbow, and so the deformation of the skin surface introduce secondary motions. For this reason we model the elbow joint as a generic rotational joint.

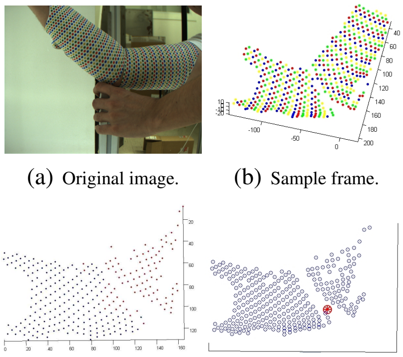

(a) Original image. (b) Sample frame.

(c) LSA segmentation. (d) Estimated Joint.

Figure 11: The second experiment setup. The images show: a) a sample frame, b) a reconstructed frames, c) the segmentation result and d) the estimated rotational joint (red).

7 CONCLUSIONS

In this work we address the problem of the 3D motion segmentation of a non-rigid pair of bodies (a human arm and forearm) connected by a rotational joint. In such regard we develop all the stages of the motion segmentation procedure from the acquisition to the joint parameters estimation. The main novelty of the presented approach resides in the 3D point matching stage which has to cope with soft tissue artifacts in the data. The multi camera facility is able to estimate the position in 3D space of each marker with an accuracy of about 0.5*mm* and a maximum resolution of 5 markers per square centimeter. The 95% ellipse of uncertainty associated with each marker location is estimated taking into account both the setup intrinsic/extrinsic parameters and the accuracy of the markers acquired images. We also carried out an evaluation of standard motion segmentation algorithm in the case of articulated bodies which present soft-tissue artifacts. The LSA approach is the best performing method for the test case showed in this work but more experimental evidence is required to asses the algorithms with different body parts.

To evaluate the localization of the joint we used both the human arm sequence and the sequence of two bodies constrained by a rotational joint. In the latter case the outcome was an accurate estimation of the joint location. In the first case we performed two relative motions between arm and forearm. When the wrist rotates together with the elbow the joint estimation as a single degree of freedom constraint failed to estimate the correct location of the elbow. This can be easily explained due to the complex relative motion involving at least two degrees of freedom. When the wrist is held at a constant attitude with respect to the elbow the joint was correctly estimated.

REFERENCES

Boujou (2009). Boujou. http://www.vicon.com/boujou/.

Corazza, S., Mündermann, L., and Andriacchi, T. (2007). A framework for the functional identification of joint centers using markerless motion capture, validation for the hip joint. *Journal of Biomechanics*, 40(15):3510–3515.

De Cecco, M., Pertile, M., Baglivo, L., Lunardelli, M., Setti, F., and Tavernini, M. (2009). A unified framework for uncertainty, compatibility analysis and data fusion for multi-stereo 3d shape estimation. *IEEE Transactions on Instrumentation Measurements*. Accepted for publication.

Fayad, J., Del Bue, A., Agapito, L., and Aguiar, P. (2009). Human body modelling using quadratic deformations. In *7th EUROMECH Solid Mechanics Conference, Lisbon, Portugal*.

Fayad, J. K. and P. M. Q. Aguiar, A. D. B. (2009). A weighted factorization approach for articulated motion modelling. In *Multibody Dynamics 2009, Warsaw, Poland*, volume 2, pages 1110–1115.

Fischler, M. A. and Bolles, R. C. (1987). Random sample consensus: A paradigm for model fitting with applications to image analysis and automated cartography. In Fischler, M. A. and Firschein, O., editors, *Readings in Computer Vision: Issues, Problems, Principles, and Paradigms*, pages 726–740. Los Altos, CA.

Ioannidis, D., Tzovaras, D., Damousis, I. G., Argyropoulos, S., and Moustakas, K. (2007). Gait recognition using compact feature extraction transforms and depth information. *IEEE Transactions on Information Forensics and Security*, 2:623–630.

Kanatani, K. (1996). *Statistical optimization for geometric computation: theory and practice*. Elsevier Science Inc. New York, NY, USA.

Scholz, V. and Magnor, M. (2006). Multi-view video capture of garment motion. *Proceedings of IEEE Workshop on Content Generation and Coding for 3D-Television*, pages 1–4.

Tresadern, P. and Reid, I. (2005). Articulated structure from motion by factorization. In *Proc. IEEE Conference on Computer Vision and Pattern Recognition, San Diego, California*, volume 2, pages 1110–1115.

Tron, R. and Vidal, R. (2007). A benchmark for the comparison of 3-d motion segmentation algorithms. In *IEEE conference on computer vision and pattern recognition*, volume 4.

Vidal, R., Ma, Y., and Sastry, S. (2005). Generalized principal component analysis (gpca). *IEEE Transactions on Pattern Analysis and Machine Intelligence*, 27(12):1945–1959.

White, R., Crane, K., and Forsyth, D. (2007). Capturing and animating occluded cloth. *ACM Transaction on Graphics*.

Yan, J. and Pollefeys, M. (2008). A factorization-based approach for articulated non-rigid shape, motion and kinematic chain recovery from video. *IEEE Transactions on Pattern Analysis and Machine Intelligence*, 30(5).